Thermochimica Acta, 119 (1987) 301–310
Elsevier Science Publishers B.V., Amsterdam – Printed in The Netherlands

CALORIMETRIC DETERMINATION OF ENTHALPY CHANGES IN OCTYLCYANOBIPHENYL (8CB) LIQUID CRYSTAL TRANSITIONS

E. ROJAS and J. SALAN

Departament de Termologia, Facultat de Física de la U.B. Diagonal, 645 08028 Barcelona (Spain)

E. CESARI

Departament de Física, Facultat de Ciències, Universitat de les Illes Balears, Ctra. de Valldemossa Km 7.5 07071 Palma de Mallorca (Spain)

J. FONT, J. MUNTASELL and J.Ll. TAMARIT

Departament de Física, E.T.S.E.I.B., U.P.C. Diagonal, 647 08028 Barcelona (Spain)

(Received 18 February 1987)

ABSTRACT

A specially designed differential scanning heat-flux calorimeter is used for the determination of enthalpy changes in the transitions between mesophases of the octylcyanobiphenyl (8CB) liquid crystal. Latent heats can be separated from pre-transitional effects in certain cases and higher-order transitions can be well identified experimentally.

INTRODUCTION

Liquid crystals are substances which have a great variety of intermediate phases between the isotropic liquid and the crystal phases. The different kinds of transitions between these mesophases are very interesting as they allow the verification of some general theories about phase transitions [1]. Some of these are first-order transitions (existence of a latent heat) while in other transitions there are discrepancies between the theoretical and experimental results [2,3] owing to the presence of small latent heats.

A first-order transition involves a discontinuity in the specific heat c at the transition temperature T_t so that the approximation limits of C_p at T_t are different. Because of this fact there is a discontinuity in the enthalpy values at T_t equal to

$$L = \left(C_p^+ - C_p^-\right)T_t \tag{1}$$

where L is the latent heat and C_p^+ and C_p^- are the limiting values of C_p in the two phases at T_t obtained by extrapolation.

0040-6031/87/$03.50

Suitable values of L can be obtained from C_p measurements when $\Delta C_p/\Delta T$ near T_t in the two phases is approximately constant. If there are important divergences of C_p (owing to pre- and post-transitional effects) in any phase, C_p^+ and C_p^- values are less well defined at T_t. Therefore L values obtained from eqn. (1) may not have much meaning. In these cases the range of extrapolation, which depends on the technique used for C_p measurements, must be as narrow as possible.

Using typical methods of C_p measurements we cannot reach temperatures sufficiently near T_t (adiabatic pulse type calorimeter [4]) and also we cannot obtain absolute C_p values with good accuracy (isoperibolic pulse calorimetry [5] and a.c. calorimetry [6,7]). However, depending on the thermal properties, the size and the shape of the sample, some of these techniques are not available.

By direct measurement of L using scanning calorimetry techniques such as DTA [8], DSC [9] and scanning adiabatic calorimetry [10] it may be difficult to distinguish L from enthalpy changes corresponding to divergences of C_p near T_t. When the scanning rate β is reduced, these difficulties are less severe, but the response of the device has a poor resolution unless greater sample masses are used.

There are doubts about the existence of latent heats in some transitions of liquid crystals as in the case of the liquid crystal octylcyanobiphenyl (8CB). This has a low thermal diffusivity (10^{-3} cm^2 s^{-1}), typical of these materials, which represents another experimental difficulty.

In this work we analyse the processes crystal–smectic A–nematic–isotropic liquid, taking place in the range 0–50 °C, corresponding to the 8CB, by means of a differential scanning heat-flux calorimeter specially designed for working at very slow scanning rates. The sensors have a sufficiently high sensitivity to allow us to obtain good resolution even for small mass samples (0.1 g). Small samples are desirable in order to minimize the thermal gradients in the sample working under dynamic conditions, owing to the low thermal diffusivity.

EXPERIMENTAL

Description of the device

We used a heat-flux microcalorimeter [11] for these measurements. The ΔT signal was detected by two thermoelectric modules (Melcor FC06-32-06L) in opposition. We acquired ΔT signal (without amplification) through a microvoltmeter HP 3478A (100 nV resolution) for calibration and kinetic identification and a Keithley 181 nanovoltmeter (10 nV resolution) for measurement runs. The temperature signal (T) was measured with a Solartron 7081 multimeter (10 nV resolution). Numerical data acquisition

was performed via IEEE-488 with a sampling of 3 values s^{-1}. The temperature control system consisted of an electrical resistance surrounding the calorimeter. For the cooling runs we placed the calorimeter in a Dewar with a cryogenic liquid. We also used a thermostatic bath (Haake N3, 0.01 K resolution) that allowed us to obtain very slow scanning rates.

Calibration

A constantan electric resistance (0.05 mm diameter) was used to calibrate our experimental system using Joule's effect. The resistance was about 60 Ω and a current of 25 mA flowed for 10 s. The calibration was performed for two different configurations in order to study the behaviour of the system under very different experimental conditions. In configuration A the electrical resistance was placed in an aluminium crucible (6 mm diameter, 2.7 mm height, 35 mg mass). In configuration B we used a glass crucible (8 mm diameter, 5 mm height, 350 mg mass). We carried out the calibration in the temperature range −30 to 80 °C. The evolution of the sensitivity with temperature was given by the following expressions for the two configurations. For configuration A

$$k = -5.19 \times 10^{-3}\, T^2 + 3.752\, T - 304.7$$

i.e. $k = 353.8$ mV W^{-1} for $T = 300$ K where k (mV W^{-1}) is the sensitivity. The correlation coefficient r is 0.9978. For configuration B

$$k = -5.21 \times 10^{-3}\, T^2 + 3.518\, T - 291.1$$

i.e. $k = 295.4$ mV W^{-1} for $T = 300$ K and $r = 0.9988$.

Both cases show a sensitivity 30 times the sensitivity of a typical DTA with the same output register.

Kinetic identification

We have carried out the kinetic identification of our system using the standard inverse filtering and harmonic analysis techniques [12,13]. In Tables 1 and 2 we include the poles (p) and zeros (z) of the transfer function determined by inverse filtering. As we can see in these tables, the kinetics of our system do not change appreciably in the range of temperatures studied. In the determination of the poles, the derivation step used has been $3\Delta t$, $2\Delta t$ and Δt (Δt, sampling period) for the first, second and following poles respectively. Because there are no problems of noise in the identification of the zeros, we have always employed an integration step equal to Δt. The existence of zeros in the the transfer function makes possible the identification of four and three time constants (for configurations A and B respectively) with good resolution owing to the attenuation that occurs in the numerical integration.

TABLE 1

Time constants ($\tau = -1/p$, $\tau^* = -1/z$, p = pole and z = zero) determined by inverse filtering for the configuration A

T (°)	τ_1 (s)	τ_2^* (s)	τ_2 (s)	τ_3 (s)	τ_2^* (s)	τ_4 (s)
−30	14	12	5	4.5	3.5	0.5
−3	14	12	6	3.8	3.25	< 0.3
27	14	11	5.2	4	2.85	0.4
37	13.5	9.8	5	4.1	3	0.5
50	13	10	5.2	4.6	3.3	0.5
68	13.5	8.5	5	3	2.1	0.4

TABLE 2

Time constants ($\tau = -1/p$, $\tau^* = -1/z$, p = pole and z = zero) determined by inverse filtering for the configuration B

T (°C)	τ_1 (s)	τ_2 (s)	τ_1^* (s)	τ_3 (s)
−27	26	4.4	3.25	1.25
−10	26	4.2	2.75	0.8
1	26	4.2	2.70	0.8
26	26	4.6	3.1	1.4
46	25.5	4.6	2.8	0.9
67	24.5	4.4	2.4	0.7

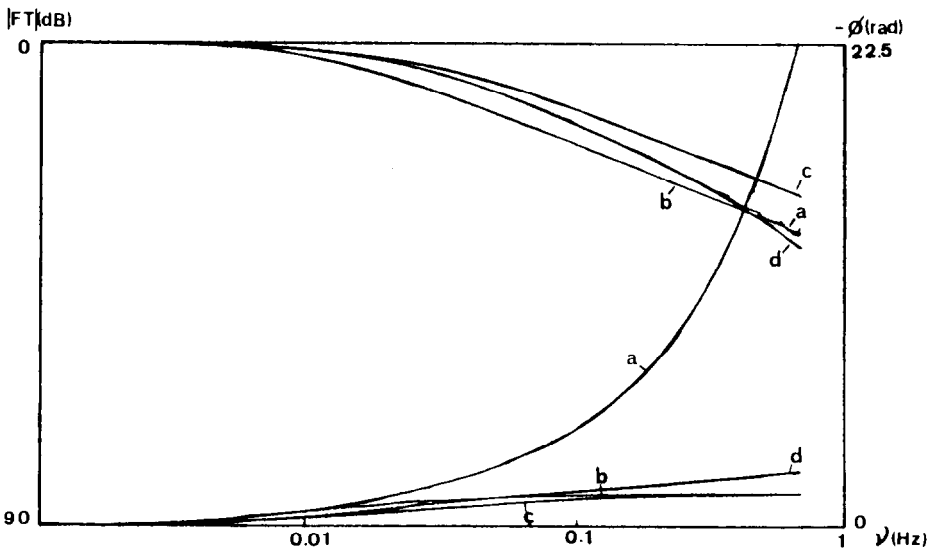

Fig. 1. Transfer functions (modules and phases) for configuration A ($\tau^* = -1/z$, $\tau = -1/p$): curves a, experimental; curves b, $\tau_1 = 14$ s; curves c, $\tau_1 = 14$ s, $\tau_1^* = 11$s, $\tau_2 = 5.2$ s; curves d, $\tau_1 = 14$ s, $\tau_1^* = 11$ s $\tau_2 = 5.2$ s, $\tau_3 = 4$ s, $\tau_2^* = 2.85$ s. (Curves a, harmonic analysis; curves b, c, d, inverse filtering.)

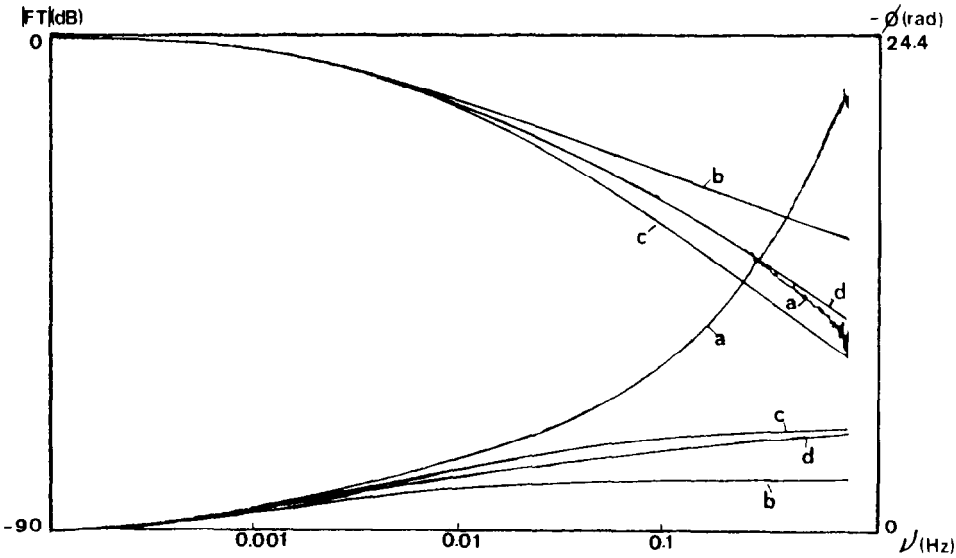

Fig. 2. Transfer functions (modules and phases) for configuration B ($\tau^* = -1/z$, $\tau = -1/p$): curves a, experimental; curves b, $\tau_1 = 26$ s; curves c, $\tau_1 = 26$ s, $\tau_2 = 4.6$ s; curves d, $\tau_1 = 26$ s, $\tau_2 = 4.6$ s, $\tau_1^* = 3.1$ s, $\tau_3 = 1.4$ s. (Curves a, harmonic analysis; curves b, c, d, inverse filtering.)

In Figs. 1 and 2 we represent the transfer functions (modules and phases) obtained by harmonic analysis corresponding to a temperature of 30 °C. These figures show that the transfer functions are well established up to a frequency of 0.70 Hz (configuration A) and 0.35 Hz (configuration B). We also include in Figs. 1 and 2 the partial transfer functions identified by inverse filtering under the same conditions.

Figures 1 and 2 show that there is good concordance between the transfer functions determined by harmonic analysis and inverse filtering up to 0.4 Hz (configuration A) and 0.2 Hz (configuration B). Both identification techniques prove that our system, with configuration B, has a main time constant of approximately 26 s, including sample and glass crucible. If it were possible to use a metallic crucible, this characteristic time would be half the previous time. This difference emphasizes the dynamic importance of the addendas to our system. In the worse case, we accept that the ΔT signal is completely released 3 min after the end of the thermal effect. However, the great sensitivity of our calorimeter makes possible measurements with very slow scanning rates (about 10^{-3} K min^{-1}) and with good resolution. The values of the release time and the sensitivity enable our device to study samples with small thermal diffusivities.

We need to employ the above glass crucible because the liquid crystal 8CB etches the aluminium. The sample mass is about 100 mg.

RESULTS AND DISCUSSION

The liquid crystal 8CB presents three transitions between the crystal and the isotropic liquid phases: crystal–smectic A–nematic–isotropic liquid. These transitions are represented in Figs. 3–5. We include in Tables 3–5 the enthalpy changes (ΔH) and temperatures corresponding to these processes.

Crystal–smectic A transition. We studied the crystal–smectic A transition (see Table 3) using heating rates of about 0.1 K min^{-1}. The signal-to-noise ratio is approximately 90 dB. In Fig. 3 we observe that the return to the baseline (smectic A phase) is more rapid than the departure from the baseline (crystal phase).

Since the experimental system kinetics are the same in all the endothermic processes, the slow evolution of ΔT at the beginning of the process can be imputed to pre-transitional effects in the crystal phase.

Smectic A–nematic transition. The scanning rates used for these measurements (see Table 4) are in the range 10^{-3}–0.2 K min^{-1}. The ΔT signal for this process is very small having a signal-to-noise ratio of 35 dB for $\beta = 0.2$ K min^{-1}. All the thermograms present a distinctive shape (Fig. 4) which does not change appreciably with the scanning rate.

Nematic–isotropic liquid transition. The scanning rate employed are in the range 10^{-3}–0.2 K min^{-1}. The signal-to-noise ratio is 70 dB for $\beta = 0.1$ K min^{-1} (see Table 5). We observe light pre-transitional effects in the nematic phase before the break point where the latent heat appears, corresponding to a first-order process (Fig. 5). When the scanning rate is reduced, pre-transitional effects merge into the baseline of the thermogram.

Owing to the great sensitivity of our experimental system, we have been able to analyse the shape of the thermograms corresponding to the transitions nematic–isotropic liquid and smectic A–nematic using very slow scanning rates. Under these conditions, and taking into account the small release time of our device, it is possible to determine the ΔH values for first-order processes and/or the evolution of C_p, not measurable with

TABLE 3

Typical ΔH values from several runs with different scanning rates (β) for the crystal–smectic A transition ($T_i - T_j$, temperature interval for integration of peak area)

ΔH (kJ mol^{-1})	$T_i - T_j$ (°C)	β (°C min^{-1})	Reference
29.19	19.0–22.7	0.1	This work
29.15	19.8–22.9	0.095	This work
29.30	19.3–22.3	0.074	This work
29.1 ± 1.0	17.2–22.0	about 0.001	2
25.3 ± 0.1	24	5	14
25.3	21	–	15
23	21.1	–	16

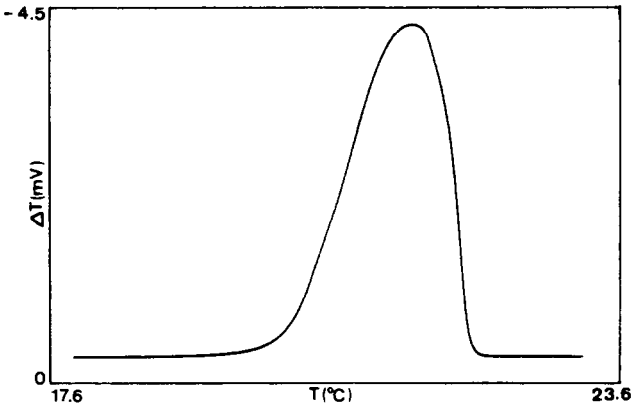

Fig. 3. Crystal → smectic A transition for $\beta = 0.1$ K min^{-1}.

TABLE 4

Typical "ΔH" values associated with the peak of smectic A–nematic transition from several runs with different scanning rates (β) ($T_i - T_j$, temperature interval for integration of peak area)

"ΔH" (kJ mol^{-1})	$T_i - T_j$ (°C)	β (°C min^{-1})	Reference
0.098	34.1–32.0	−0.13	This work
0.102	31.8–33.1	0.026	This work
0.014	33.0–33.1	0.0028	This work
0.021	32.6–32.8	0.0019	This work
0.019	32.6–32.8	0.0012	This work
0.218	31–37	about 0.001	2
0.13	34	5	14
0.126	32	–	15
0.2	33.5	–	16

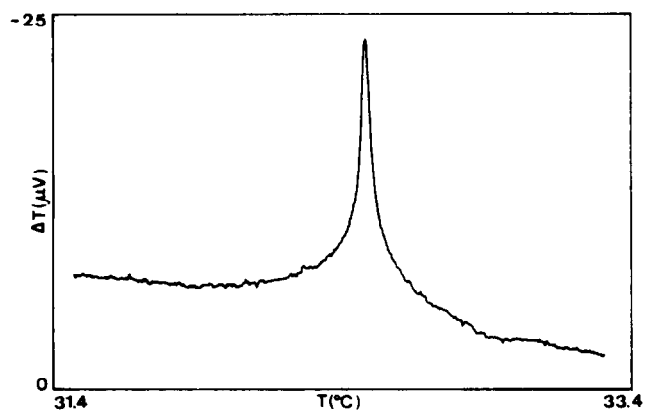

Fig. 4. Smectic A → nematic transition for $\beta = 0.026$ K min^{-1}.

TABLE 5

Typical ΔH values from several runs with different scanning rates (β) for the nematic–isotropic liquid transition ($T_i - T_j$, temperature interval for integration of peak area)

δH (kJ mol^{-1})	$T_i - T_j$ (°C)	β (°C min^{-1})	Reference
0.711 [a]	39.5–40.6	0.15	This work
0.605 [b]	39.8–40.4	0.15	This work
0.763 [a]	39.6–40.7	0.11	This work
0.613 [b]	40.0–40.5	0.11	This work
0.750 [a]	39.7–38.5	−0.019	This work
0.631 [b]	39.7–39.5	−0.019	This work
0.674 [a]	40.2–39.7	−0.006	This work
0.615 [b]	40.2–40.1	−0.006	This work
0.631	39.7–39.2	−0.003	This work
0.597	39.9–39.7	−0.0012	This work
0.595	39.9–39.7	−0.0013	This work
0.612 ± 0.005		about 0.001	2
0.97 ± 0.08	42	5	14
0.878	40	–	15
0.7	40.5	–	16

[a] These values include the pre-transitional effect and latent heat.
[b] Value associated with the latent heat for the same peak.

conventional DTA or DSC systems. In Figs. 6 and 7 we represent the processes isotropic liquid → nematic and smectic A → nematic for $\beta = 1.1 \times 10^{-3}$ and 1.7×10^{-3} K min.

The change in the shape of the thermograms for the isotropic liquid–nematic transition (Figs. 5 and 6) when the scanning rate decreases is typical for first-order processes. However, for the smectic A–nematic transition (Figs. 4 and 7) the ΔT signal decreases with the scanning rate, but we do not observe any change in the shape of the peak. Also the peak area for

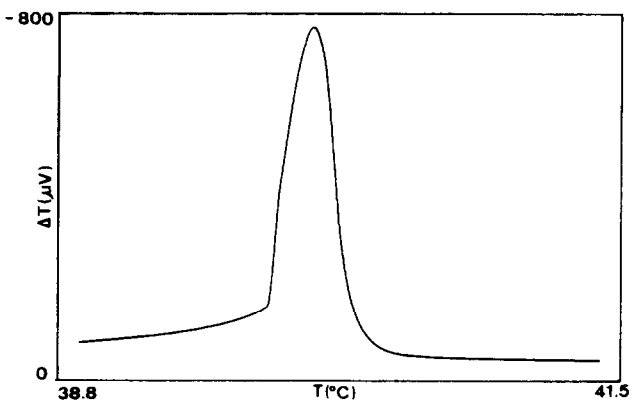

Fig. 5. Nematic → isotropic liquid transition for $\beta = 0.15$ K min^{-1}.

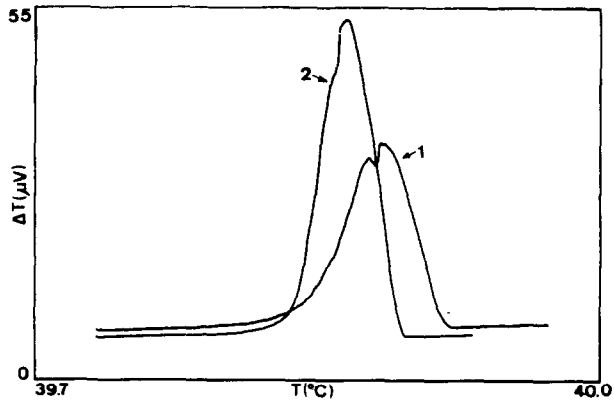

Fig. 6. Isotropic liquid → nematic transition for $1 \rightarrow \beta = -1.1 \times 10^{-3}$ K min^{-1} and $2 \rightarrow \beta = -1.7 \times 10^{-3}$ K min^{-1}.

the smectic A–nematic transition depends strongly on the scanning rate (see ΔH values in Table 4). Because of these facts we think that the smectic A–nematic may be a higher-order transition. The shape of these thermograms, typical for higher-order transitions are very similar to the evolution of C_p obtained by means of adiabatic and a.c. calorimetry [2,17,18].

The results described in this paper clearly show that our experimental system, in spite of its simplicity, is very suitable for studying these kinds of transitions in liquid crystals because of the high sensitivity and fast response.

Pre-transitional effects in first-order transitions can be evaluated or their contribution to the total enthalpy changes (depending on the scanning rate)

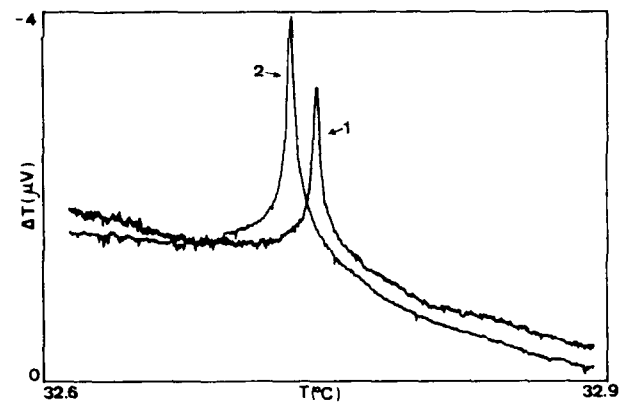

Fig. 7. Smectic A → nematic transition for $1 \rightarrow \beta = 1.1 \times 10^{-3}$ K min^{-1} and $2 \rightarrow \beta = 1.7 \times 10^{-3}$ K min^{-1}.

minimized. This is another reason for the good accuracy of the latent heat measurements.

ACKNOWLEDGEMENT

One of us (E. R.) acknowledges financial support from C.A.I.C.Y.T. n.PR83-2606.

REFERENCES

1 K.G. Wilson, Rev. Mod. Phys., 55 (1983) 583.
2 J. Thoen, H. Marynissen and W. Van Dael, Phys. Rev. A, 26 (1982) 2886.
3 H. Marynissen, J. Tohen and W. Van Dael, Mol. Cryst. Liq. Cryst., 124 (1985) 195.
4 H. Suga and S. Seki, Bull. Chem. Soc. Jpn., 38 (1965) 1000.
5 R.L. Fagaly and R.G. Bohn, Rev. Sci. Instrum., 43 (1977) 1502.
6 P.F. Sullivan and G. Seidel, Phys. Rev., 173 (1968) 679.
7 P.R. Garnier and M.B. Salamon, Phys. Rev. Lett., 26 (1971) 1523.
8 M.M. Faktor and R. Hanks, Trans. Faraday Soc., 63 (1967) 1122.
9 M.J. O'Neil, Ann. Chem., 36 (1964) 1245.
10 J.A. Lipa, C. Edwards and M.J. Buckingham, Phys. Rev. A, 15 (1977) 778.
11 J.L. Macqueron, G. Sinicki and R. Bernard, C.R. Acad. Sci., Ser. B, 266 (1968) 1.
12 E. Cesari, V. Torra, J.L. Macqueron, R. Prost, J.P. Dubes and H. Tachoire, Thermochim. Acta, 53 (1982) 1.
13 E. Cesari, V. Torra, J.L. Macqueron, R. Prost, J.P. Dubes and H. Tachoire, Thermochim. Acta, 53 (1982) 17.
14 G.W. Smith, Mol. Cryst. Liq. Cryst. Lett., 41 (1977) 89.
15 L. Liebert and W.B. Daniels, J. Phys. (Paris) Lett., 38 (1977) L-333.
16 A.J. Leadbetter, J.L.A. Durrant and M. Rugman, Mol. Cryst. Liq. Cryst. Lett., 34 (1977) 231.
17 K.J. Lushington, G.B. Kasting and C.V. Garland, Phys. Rev. B, 22 (1980) 2569.
18 C.V. Garland, Thermochim. Acta, 88 (1985) 127.